Effect of [Tris(trimethylsiloxy)silyethyl]dimethylchlorosilane on the Corrosion Protection Enhancement of Hydrophobic Film Coated on AISI 304

A. D. Baruwa[1,], E. T. Akinlabi[1], O. P. Oladijo[2, 1], N. Maledi[3] and J. Chinn[4]*

[1] Department of Mechanical Engineering Science, University of Johannesburg, South Africa
[2] Department of Chemical, Material and Metallurgical Engineering, Botswana International University of Science and Technology, Botswana
[3] School of Chemical and Metallurgical Engineering, University of the Witwatersrand, South Africa
[4] Integrated Surface Technologies Inc. 1455 Adams Drive, Suite 1125, Menlo Park, California 94025, United States

[*]E-mail: darebaruwa@gmail.com

The effects of Organofunctional moieties and the adhesion properties of hydrophobic [Tris(trimethylsiloxy)silyethyl]dimethylchlorosilane (Alkyl)] coated on AISI 304 to determine the corrosion resistance were investigated and presented. Two different types of adhesion, namely: silicon oxide and plasma silicon oxide films were grown on AISI 304 with the aid of an atomic-layer deposition technique. The effects of the surface preparations on the functionality and the properties of the hydrophobic silane coating were characterized, using the scanning electron microscope (SEM) and the atomic force microscope (AFM) for morphology and topography. X-ray diffraction (XRD) and attenuated Fourier-transform infrared (FTIR-ATR) were used for the chemical composition and the bonding structure, the water contact angle were measured and processed, as well as the determination of electrochemistry of the coated and uncoated surfaces. The results showed that the silicon oxide treated surface improved the durability of the silane film in the corrosive medium; and that has more chemical stability with the coating, when compared with the plasma silicon oxide and base material, which was distinctly discussed.

Keywords: AISI 304; corrosion; hydrophobic coating; silane; surface characterization.

1. INTRODUCTION

The surface treatment has become the basis of the performance and/or the durability of a material in an environment. Although surface treatment has been in existence for decades, its abilities are still unfolding. The surface treatment is applied in decorations, improved hardness; and it acts as an anti-corrosive layer. A surface treatment as an anti-corrosion has gained a wide appeal; as many successes have been recorded. However, many of the breakthroughs were found to have a negative impact on humans and the environments. Among the materials used for these treatments are

chromium-based coatings, VOCs and heavy metals, these can cause cancers when degraded, and they also contribute to the greenhouse effect [1]. As a consequence of these shortcomings, alternatives are currently being investigated.

The organic coating has proved to be one of the major solutions to combat the menace of corrosion. Silane is an organic compound that can function as hydrophilic, hydrophobic or superhydrophobic [2,3]. It is referred to as hydrophobic when the water contact angle is more than 90° and less than 120°. This property is harnessed with others to militate against the chemical reactions that occur on the surface of the metal, by serving as an anti-corrosion [4], anti-stiction [5], anti-reflective [6,7] for heat-pump adsorption [8]. Bera et al. [9] grafted methyl triethoxy silane (MTEO), Mercapto-propyl-triethoxy silane (MPTS) and Phenyl-amino-propyl-triethoxy silane (PAPTS) precursors into water-based glycidoxy-propyl-triethoxy silane (GPTS) for improved corrosion protection and adhesion promotion. Triethoxy(octyl)silane coating has been applied in the area of difficult combined corrosion resistance and biocompatibility, using magnesium as substrate [10]. Silane has been bonded covalently on the steel, as an improved corrosion-resistant material, using γ-glycidoxypropyltrimethoxysilane (γ-GPS), tetraethoxysilane (TEOS) and methyltriethoxysilane (MTES) as the precursors. Shen et al. [11] combined sodium dioctyl sulfosuccinate ($C_20H_37NaO_7S$), γ-aminopropyltriethoxysilane (KH550) and NaOH in using silane for anti-corrosion and cytocompatibility. Additionally, most of the substrate may not give strict adherence to the coating without treatment (activation) or the functionalizing of such surfaces [12]. Many methods have been used to address most interfacial-surface problems of metals, such as, thermal treatment [13], aqueous sodium silicate alkali solution treatment [9], grit blasting, laser ablation, water-jet and chemical attack (deserted) [14].

Recently, the treatment of a metal surface has also been used as the adhesion agent between the substrate and the coating [15]. The durability and barrier capability of any coating material is dependent on the adhesion between the substrate and the coating [16]. Silicon oxide was used as treatment and as adhesion on titanium [15,17]. The atomic-layer deposition (ALD) of silicon oxide has been shown to be a significant barrier against oxygen and moisture diffusion[18]. Plasma-silicon oxide treatment has also found application in steel coating [19]. Plasma silicon oxide is a water-insoluble compound, which can be grown on both conducting and insulating substrates [20]. Plasma-silicon oxide is also referred to as oxygen plasma, which is used to pre-treat the surface of a metal before the deposition, by removing carbonaceous contaminants [21]. It has been shown to be an adhesion strengthening and promoter [22]. Ulman [23] used oxygen plasma and water to treat the surface of a semiconductor, in order to produce hydroxyl groups that assist in perfect bonding with chlorosilane.

This work aims to study the effect of the surface pretreatment on the chemical stability and anti-corrosion capability of the newly developed hydrophobic [Tris (trimethylsiloxy)silyethyl]dimethylchlorosilane.

2. EXPERIMENTAL

2.1 Materials

Commercially available AISI 304 stainless steel 3mm thickness was cut into 100 X 100 mm for coating and easy delivery into the chamber. [Tris(Trimethylsiloxy)silyethyl]dimethylchlorosilane (Alkyl) was produced by Integrated Surface Technologies Inc., USA, and the treatment materials were also sourced commercially. The hydrophobic silane was coated on the bare sample (AISI 304) of the plasma silicon oxide and silicon oxide pre-treated surface. The chemical structure of [Tris(Trimethylsiloxy)silyethyl]dimethylchlorosilane is shown in Figure 1.

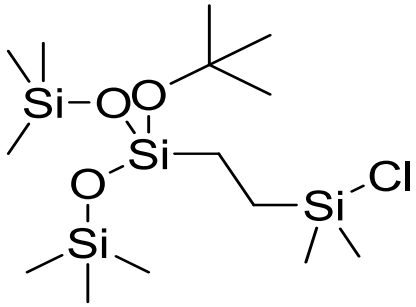

Figure 1. The chemical structure of hydrophobic Tris(Trimethylsiloxy)silyethyl]dimethylchlorosilane used for the experiment.

2.2 Steel-surface treatment

Prior to deposition, the surface of AISI 304 was ground up to 800 microns to achieve a flat surface. The surface was not polished in order for the coating to have proper adhesion to the substrate. The ground surface was cleaned using acetone, followed by ethanol, then dried under nitrogen stream, and was wrapped to avoid contaminant before deposition. The coating was laid by the RPX-540 hybrid atomic layer depositor (ALD) and the chemical vapour depositor (CVD) machine. The treatment was implemented in two-stages: using oxygen plasma/silicon oxide, followed by water plasma; and then the final deposition of the silane compound. The plasma silicon oxide/silicon oxide treatment was used to reform the surface dioxide layer; while the water-vapour (source of hydrogen) treatment is known to leave the surface of the substrate bonded to the (-OH) hydroxyl group. After that, the precursor of the organo-silane is released into the reaction chamber to react with the AISI 304 substrate. This was done in a temperature-controlled chamber of 120°C and a timing control via National Instruments' Labview, for 10minutes; while the pressure in the chamber was reduced to 4Pa. The resulting adhesion-layer thickness was approximately 20nm, as measured using ellipsometry on a reference Si wafer.

2.3 Characterization Methods

The morphology and topography of the coated and base samples were observed under Tescan Vega 8 Scanning Electron Microscope (SEM), using nano space's software; while the surface roughness was determined by using a Veeco Di3100 AFM with Nanoscope software.

The chemical stability and efficiency of the coating and AISI 304 base material were measured by X-ray diffraction (XRD) and Attenuated-Fourier Infrared (FTIR-ATR), by using a PANanalytical diffractometer and PerkinElmer 100 Spectrometer, respectively. The scanning parameters of the XRD are as follows: radiation source CuKα; wavelength (λ) equivalent to 1.5418Å at 40kV and 45mA; scan range of 5° - 90° with 3°/min speed. The ATR-FTIR was scanned at room temperature from (650-4000) cm^{-1}.

The static water contact angle was investigated using the sessile method by dropping 1µL of distilled water on the both the coated samples and the bare substrate at room temperature. Micro CCD camera was used to take the image, and the images were transferred to a suitable software for proper analysis. Average of 10 measurements were taken on each sample and average was taken to establish the water contact angle of each sample.

The electrochemical tests were conducted by using Ivium's Technologies potentiostat, with natural seawater as the electrolyte. The samples were immersed in natural seawater for 60 min to obtain OCP stability. The polarization curve was obtained at the scan rate set as $0.5mVs^{-1}$, the frequency at 10 kHz to 10 mHz, and the sinusoidal potential amplitude of ± 250mV to the OCP was used. The experiment was repeated three times for repeatability. The sample size of area 10mm X 10mm was used for the all the characterizations.

3. RESULTS AND DISCUSSION

3.1 Coating Microstructure

The morphology of the coated surfaces was examined. Four different scans were made on the samples of 10 X 10 mm for comparisons; as presented in Figures 2 (a) and (b).

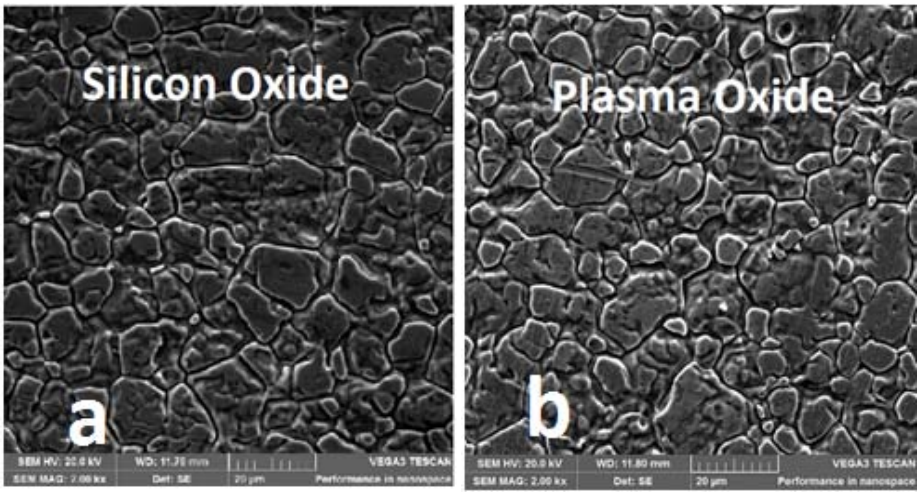

Figure 2. The SEM images of the hydrophobic alkyl coated on AISI 304 showing the same microstructural distribution without any cracks from different adhesions of (a) silicon and (b) plasma silicon oxides.

Figure 2 shows that the morphology of the alkyl in the two treatments looks similar. The big and small grains are intermingled in a district. It is evident that the coating has no micro-cracks on the surface; as can be seen in Figure 2. The lack of cracks will reduce the diffusivity of the electrolyte or the corrosive media to the substrate's surface. It also appears that the coating is prime and flat. The grain size and morphology of these two treatments do not yield any dissimilar patterns. Therefore, it is challenging to judge the efficacy of any of the treatments – without plunging into the cross-section of the film.

3.2 Atomic Force Microscopy Characterization

The Atomic force microscope (AFM) is a useful tool to determine the topography of a surface; the AFM was therefore used to probe the surface characteristics of the coated samples, with different treatments, and the coating reaction to the surface treatment/adhesion. A reference (see Figures 3a, 3b, and 3c) was captured and presented in Table 1. Five scans were made over a sample size of $1cm^2$; and the average was taken and recorded for this report. From the data captured, both surface preparations are smoother than the base material; while the silicon oxide has less roughness when compared with the plasma silicon oxide. The roughness and grain size analysis shows that the surface treatment had an impact and contributed to the smoothness and functionality of a coated surface – having prepared both samples under the same conditions (Table 1). The silicon oxide also showed a higher degree of surface homogeneity than plasma silicon oxide. There were no micro-pores visible in the coated samples, which is an indication of the lack of heterogeneity in the cross-linking of the compounds. The pores are the access gate for the diffusion of ions/water unto the substrate. Poor

crosslinking, however, generate pores which increase the uptake or permeability of water or ions that would result in delamination of the coating from the AISI 304 substrate [24,25]. This will enable the coated surface to resist the penetration of corrosive media to the substrate, and it would improve the corrosion resistance of the material [26].

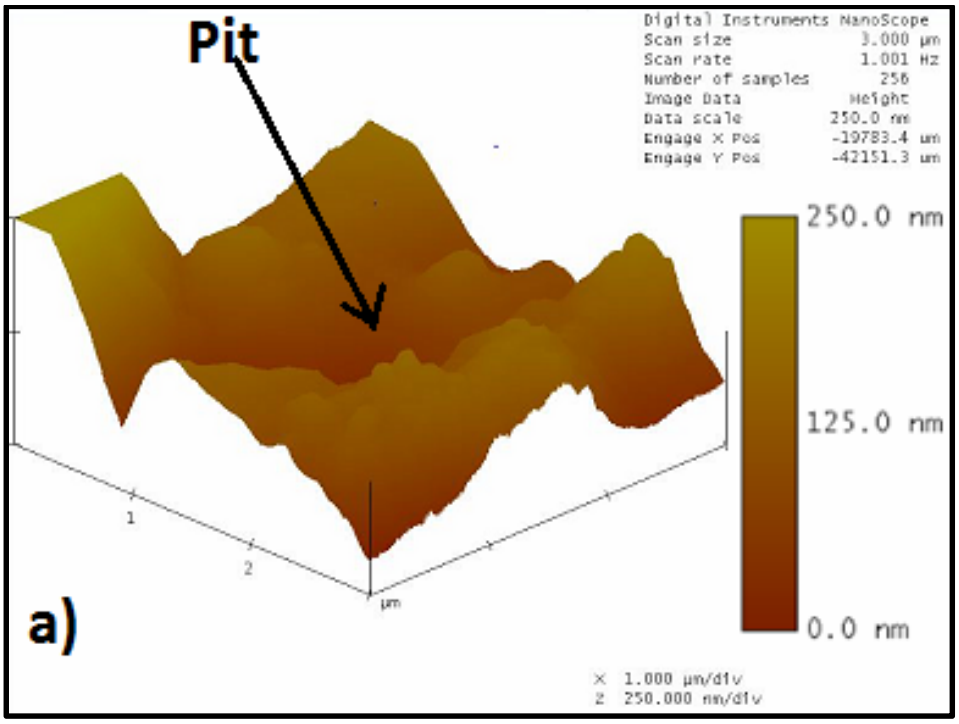

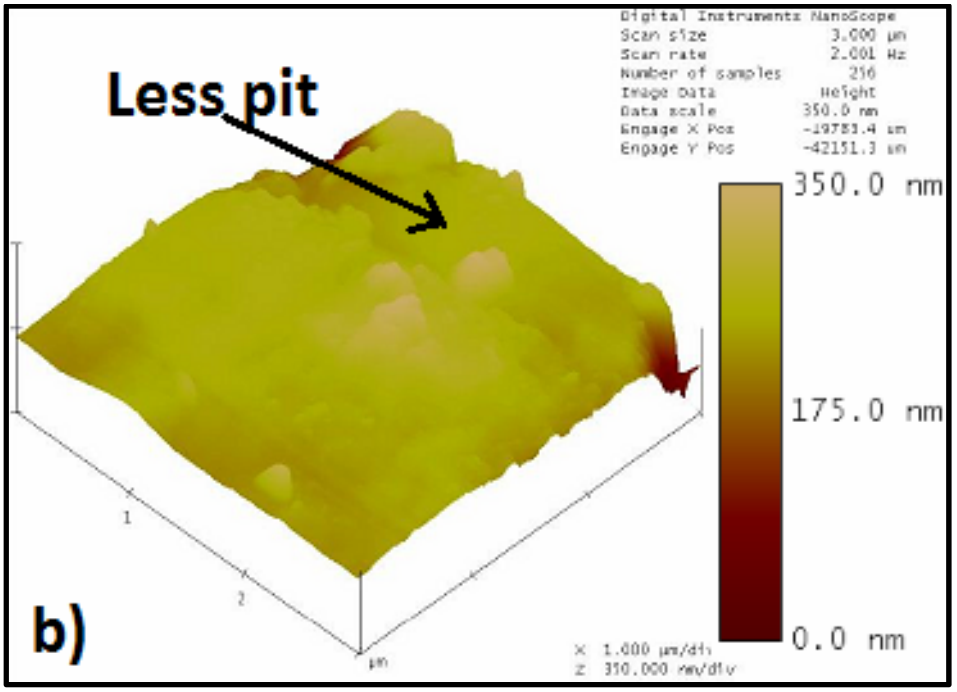

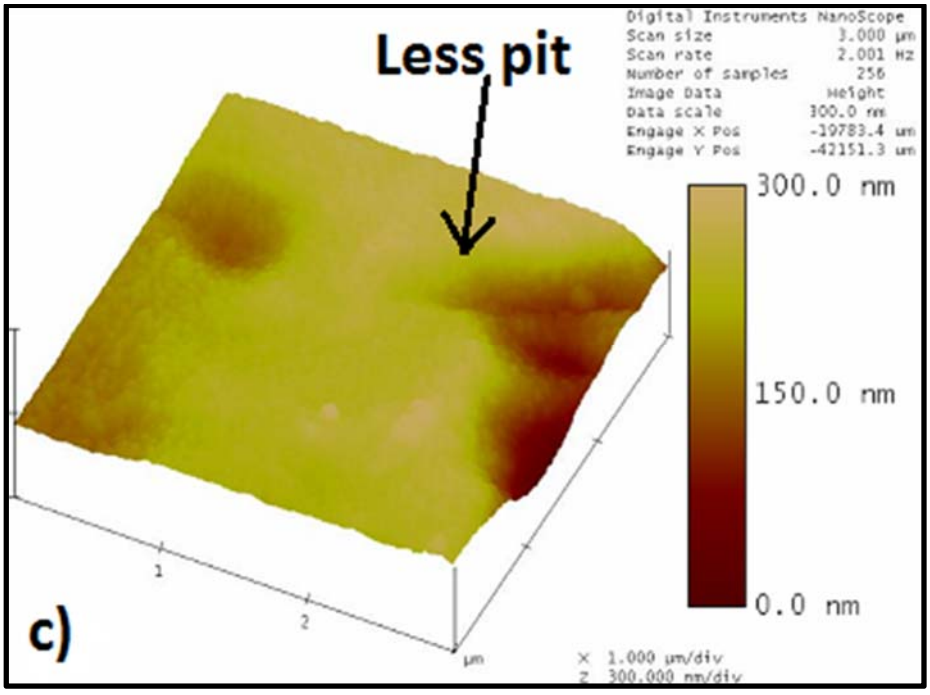

Figure 3. Shows the AFM images (3 X 3 µm^2) taken at the tapping mode, with a resonance frequency of 75 kHz of a) bare 304; b) plasma; and c) silicon oxide treatments. The coated samples show a relatively less pit surface when compared with the bare AISI 304.

Table 1. Presents the average data captured from five scans on coated samples and bare AISI 304 from the Atomic force microscope in the tapping mode.

Sample	Rms (nm)	Ra (nm)	Surface area (µm^2)	Grain Size Range (nm)
Bare	76.27±4.2	65.14±3.9	9.77±2.4	27.93-1539.48
Plasma	15.23±2.3	21.72±1.1	9.71±0.2	19.53-1438.61
Silicon	13.63±2.9	9.02±2.8	9.28±0.3	19.81-1512.32

3.3 X-ray Diffraction

The phase crystalline structures and crystallite size of the silanes (Alkyl) coated on the surface pretreated by using oxygen plasma, silicon oxide and the base material were characterized.

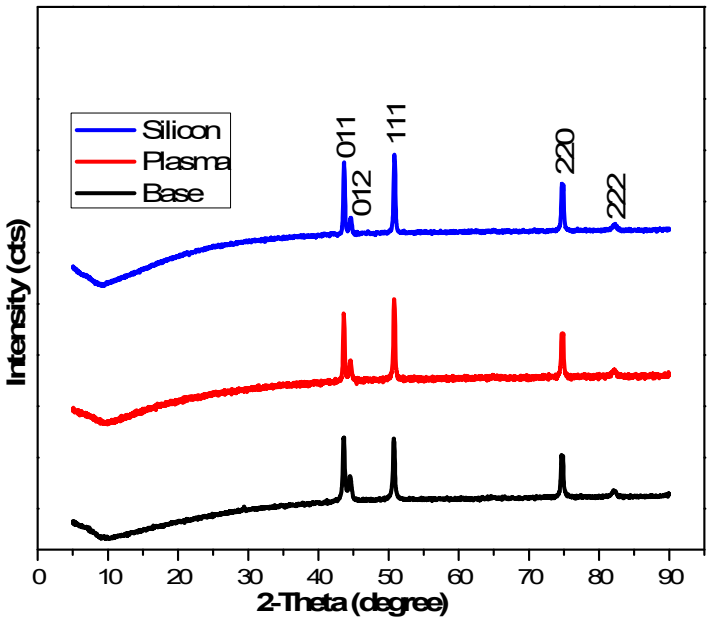

Figure 4. Depicts the XRD spectra of the base material (black), plasma silicon oxide (red), and the silicon oxide (blue) acquired at 0.0001°step. The Spectra diffraction showed no significant shift; but the differences in the elemental composition when the coated surfaces were compared with the base material.

Five peaks are associated with all the samples: with peaks at the 2-theta equivalent of 43.5°, 44.4°, 50.7°, 74.6°and 82.3°. But at 2-theta = 43.5°, the base material has a broader peak-base, when compared with the treated surface. From these peaks, the plasma and the silicon oxide treated samples diffracted Si, Fe, C, or combinations of the two; while the base material diffracted Fe only. There was an amorphous phase of Iron III fluoride at every peak, except for the base material. Furthermore, there were mixed phases at all the peaks. No shifts in the peaks of the treated samples were found compared to the base material, because of the coating thickness.

3.4 AT-FTIR Analyses

The chemical stability of the two types of treatments on the coatings was studied by using FTIR-ATR spectra. Figure 5 and Table 2 show that the two treatments present many characteristic peaks.

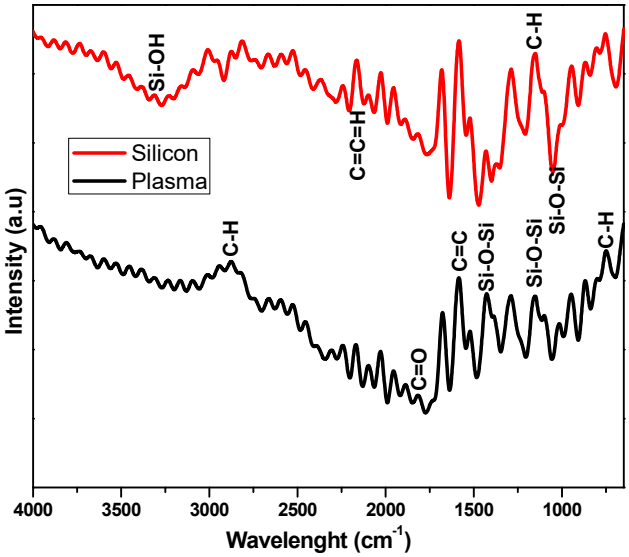

Figure 5. Presents the FTIR spectra of the organic hydrophobic-coated samples prepared by using different surface pretreatments of silicon oxide (red) and plasma silicon oxide (black) colour. Silicon oxide has Si-OH hydroxyl group which is hydrophilic in nature

There were strong Si-O-Si bending and stretching at positions 1045cm^{-1}, which was reported similarly by Aydınoğlu and Yoruç [27], 1187cm^{-1}, and 1432cm^{-1}. The associated peaks indicate that an effective protecting layer was exerted on the coated stainless steel. This is also an indication that the cross-linking of the Si-O-Si underwent complete hydrolysis. From the captured data, the frequency of the appearance of Si-O-Si is shown in the plasma silicon oxide. The presence of a broad and sharp absorption band Si-OH in axial deformation for both treatments between 3200 cm^{-1} and 4000 cm^{-1} is an indication of the formation of hydrophobic siloxane in the network of the coating during the curing process [28].

Table 2. Presents the frequencies observed after ATR-FTIR incidence on the coated samples and the peak assignment.

Peak Position (cm^{-1})	Peak assignment (Band)
600-700	C-H bending
1000-1200	Si-O-Si stretching
1300-1400	C-H bending, Si-O-Si stretching
1600-1670	C=CH axial stretching
1700-1760	C=O stretching
2000-2400	C=C=O stretching

2550-2600	S-H stretching
2900-3000	C-H (CH_2=CH_3) symmetric and asymmetric stretching
3200-4000	Si-OH broad/sharp stretching

3.5 Water Contact Angle

Water contact angle is the measurement of the degree of wettability of a surface as presented in Figure 6 and Table 2. Effect of pretreatment of silicon oxide and plasma oxide on the functionality of the silane compound was observed after 60 s of dropping distilled water on the surface. On the SiO_2 pre-treated surface, it was observed that the Silane-SiO_2 combination produced higher contact angle more than the plasma oxide and the base material. This results in a 120.7° contact angle which is in agreement with the conclusion of Pantoja et al. [29]. It could not be ascertained that the surface roughness is responsible for the high contact angle in the data acquired from AFM, but the presence of hydroxyl –OH group in the chemical spectra of the plasma oxide (from ATR-FTIR) could be responsible for the less contact angle of 102.3° observed, although, a good water contact angle has been reported for a substrate treated with plasma oxide (oxygen plasma) before deposition of superhydrophobic silane compound [30]. Besides, other factors such as particle shape or particle size could be responsible for variation in contact angle [31]. Above all, the water contact angles of both silicon oxide (120.7°) and plasma oxide (102.3°) are higher than the substrate measured as 13.6° which is an indication of successful hydrophobic surface modification.

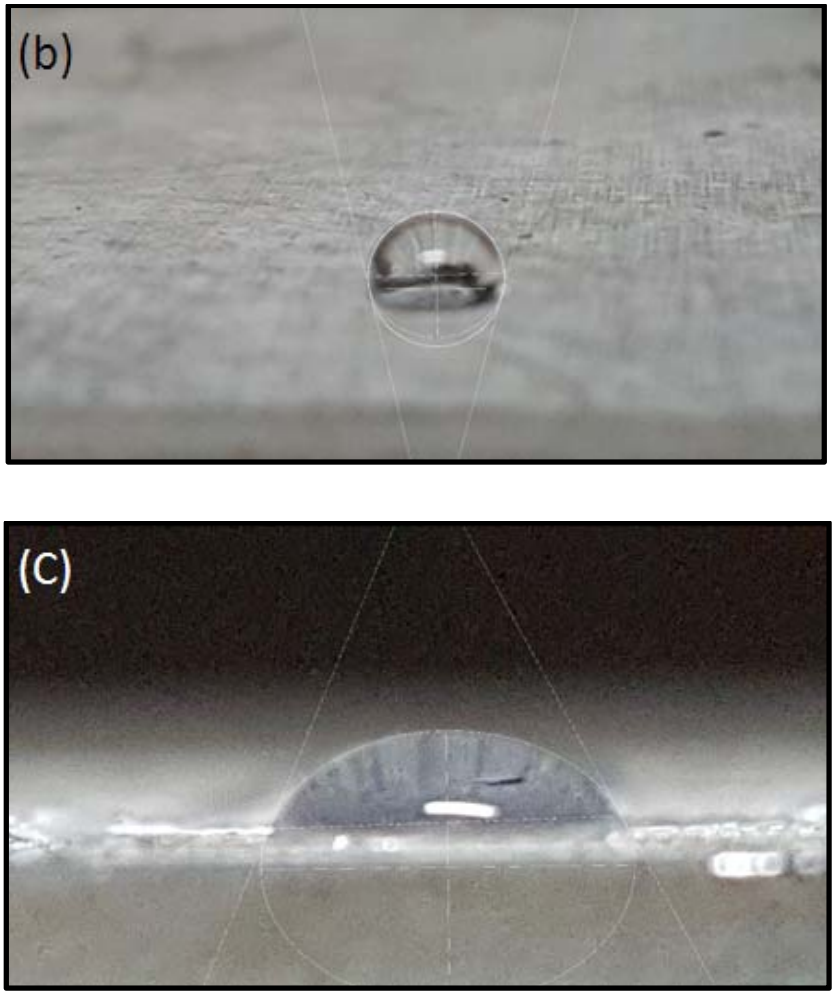

Figure 6. The distilled water contact angle measured at room temperature for hydrophobic coating of (a) plasma oxide (102.3°), (b) silicon oxide (120.7°), and (c) the base material (13.6°)

3.6 Potentiodynamic Polarization

The previous characterizations were done to ascertain the adequacy of the surface preparations/treatment and coating; but the integrity and durability of these treatments in sustaining the efficiency and functionality of the coating were tested by using potentiodynamic polarization.

From the data captured in Figure 7, the data reported in Table 3 were generated. It was observed that there was a shift in the corrosion potential of both treatments. The plasma silicon oxide pre-treated surface moved in a positive direction, forming anodic protection; while the silicon oxide shifted in a negative direction; and it formed a cathodic protection on the substrate. Although, the silicon oxide has more active corrosion potential than the plasma silicon oxide; yet the plasma silicon oxide has yielded to corrosion faster than silicon oxide, judging from the corrosion rate. This may have resulted from the corrosion tendency, based on the mixed potential theory [32,33]. It is an evidence of the confirmation of functional synergetic effect between the Fe^{2+} cations and the pre-treatment/

silane barrier property domicile in the silane compound. From the ATR-FTIR result, there are many electron rich groups such as C=CH and C=O that could chelate with Fe^{2+} cations by sharing their lone pairs in the groups' empty orbitals with Fe^{2+} cations. This forebear the formation of Fe-pre-treatment/silane complexes on the anodic site which eventually hampers the dissolution of metal. The shift of the silicon oxide towards the negative shows that the surface treatment/adhesion supported the coating by hampering the anodic dissolution of the metal into the electrolyte; and reducing the oxygen diffusion onto the surface of the AISI 304 [34].

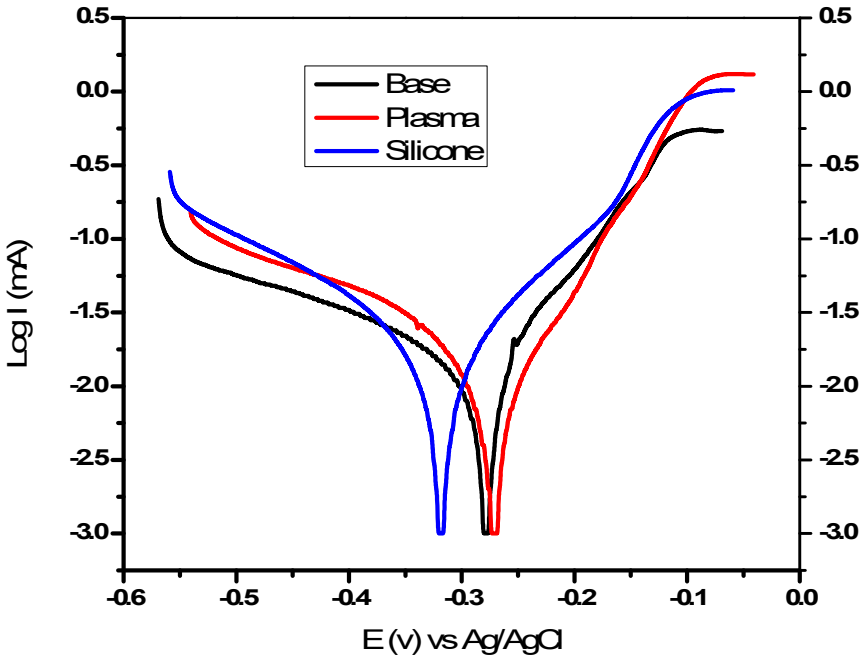

Figure 7. Depicts the potentiodynamic polarization curves of the base material (black) and the coated samples of plasma silicon oxide (red) and silicon oxide (blue) deposited by ALD and investigated in natural seawater at room temperature.

The cathodic protection of the silicon is an indication of higher electrode potential activation than the plasma silicon oxide. Table 3 shows that the current densities of both surface treatments are lower than that of the base material; and this is an indication that both preparations can reduce the corrosion rate by a barrier; while the plasma silicon oxide treatment can also alter the mechanism at which the corrosion occurs, due to its high corrosion potential. The improvement in the reduction of the currents densities means that the surfaces of the coated samples are smoother than bare AISI 304 [32,33]. The corrosion rate was significantly reduced by the order of 1 on both types of surface treatments when compared with the base material. Table 3 shows that both surface treatments display close corrosion rates. The corrosion rate was determined from the Faraday's law which relates the corrosion rate R_{Corr} or metal dissolution rate (R_M) to the corrosion current (i_{Corr}) linearly.

$$R_{corr} = \frac{KE_W}{A\rho} I_{corr} \quad (1)$$

Where E_W is the equivalent weight of the metal, ρ is the density, A is the area of the working electrode, and K is a constant. The resultant effect of the coating was measured by using the equation of Cheragi et al. [35].

$$P\% = \left(\frac{I^b_{corr} - I^c_{corr}}{I^b_{corr}}\right) \times 100\% \quad (2)$$

Where I^b_{corr} and I^c_{corr} are the current densities of the base material and the coated surfaces, respectively.

Table 3. Presents the average Potentiodynamic polarization parameters of the base metal and the coated surface obtained from the curves after 60 min immersion in pH 8.1 seawater.

	Base	Plasma silicon oxide	Silicon
E_{corr}	-0.2661	-0.2615±0.001	-0.3087±0.0009
I_{corr}	1.52E-05	7.37E-06±0.09	7.342E-6±0.14
R_p ohms	2398	3528±57	3541±21
C. rate mm/y	0.1632	0.07889±0.00003	0.07862±0.00008
P %	-	51.51	51.70

3.6 EIS Results

Electrochemical impedance spectroscopy is a useful method to determine the resistance of a material to the charge transferred through such a material. The Nyquist and Bode plots are presented below.

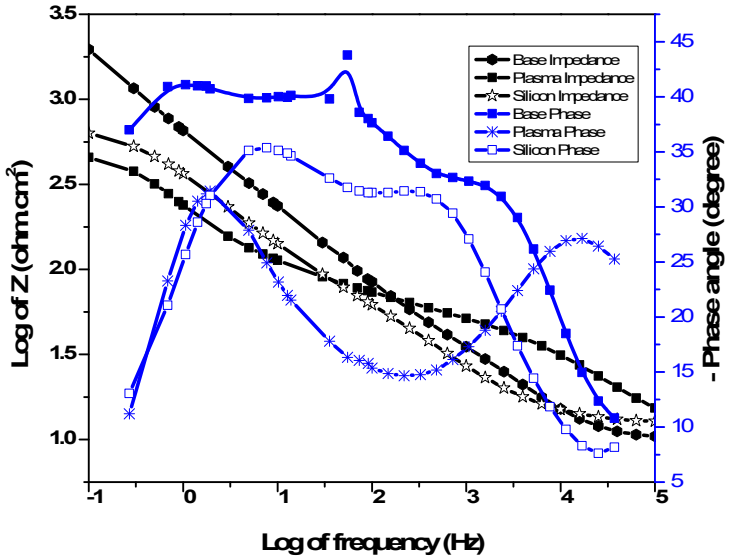

Figure 8. Depicts the Bode plot of the untreated AISI 304 and coated/treated plasma silicon oxide and silicon oxides samples measured after immersion in seawater for 60 min at room temperature.

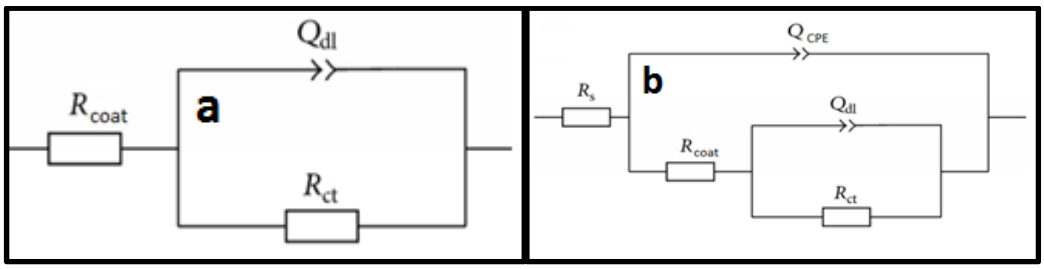

Figure 9. Shows the equivalent circuit diagram used for the fitting: a) untreated; and b) treated.

For the Bode diagram, Figure 8 was generated from the fitted electrical circuit shown in Figure 9. It is evident that the coated samples have a two-time constant (low and high frequency); while the base material has only a one-time constant. The low-frequency time constant means that the treatment/coating slows corrosion by sealing the distributed pores present in the film; and this is an indication of film compactness [25,27]. It was also revealed that the impedance and the resistance of the base material are higher than the treated surfaces at lower frequencies; but they became lowest as the frequencies and the time progressed. This means that at higher frequencies, the high chromium concentration in the stainless steel formed a considerable resistance for the corrosion mechanism to take place; but it became susceptible at a faster rate, as the time of immersion increases.

It also, means that the barrier response of the treated samples at low frequencies to the electrolyte is very high; but as time progressed it lost resistance and had a low susceptibility at high

frequencies. The larger R_{coat} or R_{pore} of averaged 128 ohms found in the silicon oxide indicates a denser and better coating compare to plasma oxide with 74 ohms.

The phase angle analysis shows that the current for both silicon and plasma silicon oxides passed through conductive pathways; because they both have low phase angles at high frequencies [37].

For qualitative assessment, the Nyquist plot was also used to access the characteristics and the capability of both treatments with reference to the base material.

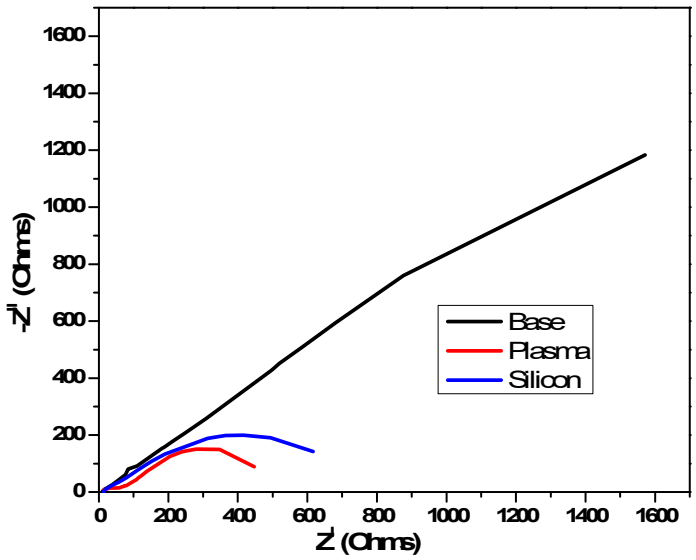

Figure 10. Depicts the Nyquist plot of the untreated and treated samples measured after immersion in seawater for 60 min at room temperature.

The Electrochemical theory posits that the corrosion rate and the resistance of the charge transfer are proportional [38]. This was proven in the work of Lin et al. [38], where the coating resistance impeded the charge transfer and barred the anodic dissolution of the coating into the solution. By using this method, it is generally accepted that the corrosion performance is based on the size of the capacitance loop. The larger the size of the capacity loop, the better the corrosion resistance ability of the material. Also, the bigger the capacity loop, the more the surface or thin film resists the electron transfer and the diffusion at the solution-metal interface. Figure 9 shows that the capacitance loop of the silicon oxide is more significant than that for the plasma silicon oxide. The span of the base material around 45° is an indication of the porous material and the possible slower rate of the diffusion process at the metal-oxide layer-metal charge transfer [39]. The capacitance loops also have wide-spread semi-circles, and the loop of the silicon oxide is more significant than that of the plasma silicon oxide; as can be seen in Figure 10. However, the loops are not perfect semicircles; and they are frequently referred to as an impedance associated with the frequency dispersion of the interfacial [40].

The resultant loops revealed that none of the surface preparations retarded corrosion via anodic or cathodic charge transfer, but by a barrier which emanated from the combination of the surface treatment and the coating chemical interaction with the treated surface. The above arguments show that the silicon oxide surface preparation is better in the corrosion resistance than the plasma silicon oxide surface preparation. This may be as a result of high water contact angle obtained from the silicon oxide pre-treated coating. The coating efficiency was calculated from the equation of Cheragi et al. [35]

$$P\% = \frac{R_{ct}^{B} - R_{ct}^{C}}{R_{ct}^{B}} \quad (3)$$

$$\theta = 1 - \frac{R_{ct}^{C}}{R_{ct}^{B}} \quad (4)$$

Where R_{ct}^{B} and R_{ct}^{C} are the resistance of the coating of the base material and the coated samples, respectively.

Table 4. Presents the parameters and their standard deviations extracted from an electrochemical test from modelling the Bode and Nyquist plots of plasma silicon oxide and silicon oxide in natural seawater.

Material	R_s(ohm)	R_{ct}(ohm)	R_{coat}(ohm)	C_{dl} (μF cm^{-2})	CPE_t Y_0 (nμF cm^{-2})	n	θ	P%
Base	109	1550			306.4	0.81		
Plasma	36±0.5	433±1.1	74±0.4	938±1.3	20±1.3	0.90	0.72	72.06
Silicon	22±0.4	604±0.7	128±0.9	1440±0.7	88±1.4	0.76	0.67	66.90

4. CONCLUSION

The effect of treatment on the functionality and the effectiveness of a coated surface was successfully investigated and reported in this paper. In the SEM analysis, the surface scan did not show the disparity in the morphology. The surface treatment might also be too thin to characterize the cross-section; as in this case, where the resultant thickness (coat plus treatment) is 20 nm. AFM indicated that the silicon oxide gave better adhesion and good chemical reaction for the smooth surface. The FTIR and XRD proved that the silicon oxide has good chemical stability when compared

with plasma silicon oxide. Higher water contact angle of silicon oxide poses to be better than plasma oxide because of the degree of repellence that aids corrosion resistance that could occurs as a result of high van-der-Waals forces that exist with stiction. The electrochemical tests manifested a robust advantage for silicon oxide over plasma silicon oxide. From all the characterizations performed on the treated samples, it is evident that the surface treatment and/or adhesion are detrimental to the aesthetic, efficiency and functionality of the coating. Also, the chemical matrix of the treatment determines the adhesion and the morphology of the coating texture.

Acknowledgement

The authors would like to thank the University of Johannesburg's Global Excellence Scholarship Board (GES) for the financial support towards achieving this publication. The equipment support by Integrated Surface Technologies (IST), USA, Microscopy and Microanalysis Unit of the University of Witwatersrand and Botswana International University of Science and Technology, Palapye are highly appreciated.

References

[1] Wahid H, Ahmad S, Nor M A M and Rashid M A, *negeri di Malaysia*, (2017) 51

[2] Nakajima A, Hashimoto K, Watanabe T, Takai K, Yamauchi G and Fujishima A, 16 (2000) 7044–7

[3] Kepler J L and Locke C E *Corrosion* (2000) 231

[4] Johansson T, Weidolf L, Popp F, Tacke R and Jurva U, *Drug Metab. Dispos.* 38 (2010) 73–83

[5] Ashurst W R, Yau C, Carraro C, Maboudian R and Dugger M T, *J. Microelectromechanical Syst.* 10 (2001) 41–9

[6] Figueira R, Fontinha I, Silva C and Pereira E, *Coatings* 6 (2016) 12

[7] Klein L C *Thin Film Process. II* (1991) 501–21

[8] Calabrese L, Brancato V, Bonaccorsi L, Frazzica A, Caprì A, Freni A and Proverbio E, *Therm. Eng.* 116 (2017) 364–71

[9] Bera S, Rout T K, Udayabhanu G and Narayan R, *Prog. Org. Coatings* 101 (2016) 24–44

[10] Gu X N, Guo H M, Wang F, Lu Y, Lin W T, Li J, Zheng Y F and Fan Y B, *Mater. Lett.* 193 (2017) 266–9

[11] Wang C, Shen J, Zhang X, Duan B and Sang J I, *J. Alloys Compd.* 714 (2017)186–93

[12] Chaffin D B and Woolley C B, *Material and Surface Coating* (2006) 1–13

[13] Hernández-Martínez D, León-Silva U and Nicho M E, *Anti-Corrosion Methods Mater.* 62 (2015)229–40

[14] Pawlowski L *The Science and Engineering of Thermal Spray Coatings* ed L Pawlowski (West Sussex, England: John Wiley& Sons, Ltd.) 2008

[15] Kotte L, Haag J, Mertens T and Kaskel S , *Metals (Basel).* 4 (2014) 639–46

[16] Felts J T *J. Plast. Film Sheeting* 9 (1993) 201–23

[17] Burton B B, Kang S W, Rhee S W and George S M *J. Phys. Chem. C* 113 (2009) 8249–57

[18] Zhang H, Guo Z, Chen Q, Wang X, Wang Z and Liu Z, *Thin Solid Films* 615 (2016) 63–8

[19] Abuali Galedari, S., Mousavi Khoei M, *J. Mech. Res. Appl.* 4 (2012) 57–61

[20] Tell B, Nahory R E, Leheny R F and De Winter J C, *Appl. Phys. Lett.* 39 (1981) 744–6

[21] DiFelice R *An investigation of plasma pretreatments and plasma polymerized thin films for titanium/polyimide adhesion,* 2001

[22] Ataeefard M, Moradian S, Mirabedini M, Ebrahimi M and Asiaban S, *Prog. Org. Coatings* 64 (2009) 482–8

[23] Ulman A F, *Chem. Rev.* 96 (1996) 1533–54

[24] Corning D A Guide to Silane Solutions: The Basics of Silane Chemistry *Dow Corning* 1–6 (2009)

[25] Sangaj N S and Malshe V C, *Prog. Org. Coatings* 50 (2004) 28–39

[26] Zandi Zand R, Flexer V, De Keersmaecker M, Verbeken K and Adriaens A, *Mater. Corros.* 67 (2016) 693–701

[27] Aydınoğlu A and Yoruç A B H,*Mater. Sci. Eng. C* 79 (2017) 382–9

[28] Longhi M, Kunsta S R, Beltrami L V R, Kerstner E K, Silva Filho C I, Sarmento V H V and Malfatti C,*Mater. Res.* 18 (2015)1140–55

[29] Pantoja M, Abenojar J and Martinez M A , *Appl. Surf. Sci.* 397 (2017) 87–94

[30] Matin A, Merah N and Ibrahim A, *Prog. Org. Coatings* 99 (2016) 322–9

[31] Chau T T, Bruckard W J, Koh P T L and Nguyen A V, A review of factors that affect contact angle and implications for flotation practice 2009

[32] Ahmad Z and Ahmad Z , (2006) 57–119

[33] Ehsani A, Moshrefi R and Ahmadi M, *J. Electrochem. Sci. Technol.* 6 (2015) 7–15

[34] Liu Y, Cao H, Yu Y and Chen S *Int. J. Electrochem. Sci.* 10 (2015) 3497–509

[35] Cheraghi H, Shahmiri M and Sadeghian Z, *Thin Solid Films* 522 (2012) 289–96

[36] Asadi N, Naderi R, Saremi M, Arman S Y, Fedel M and Deflorian F, *J. Sol-Gel Sci. Technol.* 70 (2014) 329–38

[37] Akbarinezhad E, Ebrahimi M and Faridi H R *Prog. Org. Coatings* 64 (2009) 361–4

[38] Lin M T, Wan C H and Wu W *Int. J. Electrochem. Sci.* 9 (2014) 7832–45

[39] Cooper S J, Bertei A, Finegan D P and Brandon N P *Electrochim. Acta* 251 (2017) 681–9

[40] Ghasemi O, Danaee I, Rashed G R, RashvandAvei M and Maddahy M H, *J. Cent. South Univ.* 20 (2013) 301–11